Acta Biochim Biophys Sin 2023, 55(3): 367–381
https://doi.org/10.3724/abbs.2023021
Advance Access Publication Date: 17 March 2023
Original Article

Original Article

Long noncoding RNA LINC01088 inhibits esophageal squamous cell carcinoma progression by targeting the NPM1-HDM2-p53 axis

Fan Liang[1], Qiuli Luo[2], Haibo Han[3], Jianzhi Zhang[1], Yue Yang[1,*], and Jinfeng Chen[1,*]

[1]Department of Thoracic Surgery II, Key Laboratory of Carcinogenesis and Translational Research (Ministry of Education/Beijing), Peking University Cancer Hospital & Institute, Beijing 100142, China, [2]College of Life Science and Bioengineering, Beijing University of Technology, Beijing 100020, China, and [3]Department of Clinical Laboratory, Peking University Cancer Hospital & Institute, Beijing 100142, China
*Correspondence address. Tel: +86-10-88196530; E-mail: chenjinfengdoctor@bjmu.edu.cn (J.C.) / E-mail: zlyangyue@bjmu.edu.cn (Y.Y.)

Received 10 June 2022 Accepted 30 August 2022

Abstract

Esophageal squamous cell carcinoma (ESCC) is characterized by extensive metastasis and poor prognosis. Long noncoding RNAs (lncRNAs) have been shown to play important roles in ESCC. However, the specific roles of lncRNAs in ESCC tumorigenesis and metastasis remain largely unknown. Here, we investigate LINC01088 in ESCC. Differentially expressed LINC01088 levels are screened from the GEO database. We find that LINC01088 is expressed at low level in collected clinical samples and is correlated with vascular tumor emboli and poor overall survival time of patients after surgery. LINC01088 inhibits not only ESCC cell migration and invasion *in vitro*, but also tumorigenesis and metastasis *in vivo*. Mechanistically, LINC01088 directly interacts with nucleophosmin (NPM1) and increases the expression of NPM1 in the nucleoplasm compared to that in the nucleolar region. LINC01088 decreases mutant p53 (mut-p53) expression and rescues the transcriptional activity of p53 by targeting the NPM1-HDM2-p53 axis. LINC01088 may also interfere with the DNA repair function of NPM1 by affecting its translocation. Our results highlight the potential of LINC01088 as a prognostic biomarker and therapeutic target of ESCC.

Key words esophageal squamous cell carcinoma, LINC01088, nucleophosmin, p53

Introduction

Esophageal cancer (EC) is the eighth most commonly diagnosed cancer and the sixth leading cause of cancer death worldwide [1]. Moreover, esophageal squamous cell carcinoma (ESCC) is the predominant histological subtype in China, accounting for more than 90% of all EC cases [2,3]. Despite remarkable progress in both diagnostic and therapeutic techniques over the past decades, ESCC still has a poor prognosis, and the 5-year survival rate is less than 25% [4,5]. The main reasons for this high mortality are extensive metastasis and tumor recurrence. Although various risk factors have been identified, knowledge of the genetic drivers of ESCC is still limited [6–8]. There is an urgent need to identify the molecular mechanisms underlying ESCC and to develop new and effective therapeutic approaches.

Over the past decades, aberrant expression of long noncoding RNAs (lncRNAs) has been reported to correlate with tumorigenesis and metastasis [9–11]. It was reported that the lncRNA *CASC9* promotes ESCC by recruiting EZH2 to the promoter of programmed cell death protein 4, and *HEIH* (a lncRNA) depletion slowed esophageal carcinoma cell progression by sponging microRNA-185 [12,13]. More than 90% of the human genome is functional and encodes large numbers of noncoding RNAs (ncRNAs), and lncRNAs comprise over 90% of ncRNAs [14,15]. Because of their genome-wide and tissue-specific expression patterns, lncRNAs are ideal novel biomarkers and therapeutic targets for cancer [11,15].

Zhang *et al.* [16] first reported that the expression of LINC01088 in ovarian epithelial cells (EOCs) is significantly downregulated using microarray analysis and that its expression is associated with the progression of EOC. In human non-small cell lung cancer, LINC01088 is a scaffold that recruits EZH2 to inhibit p21 expression [17]. LINC01088 physically interacts with small nuclear ribonucleoprotein polypeptide A (SNRPA) and promotes the growth and invasion of glioma cells by regulating SNRPA transcription [18]. Recently, it has also been reported that LINC01088 promotes the

apoptosis of trophoblast cells by binding with Arginase-1 and activating the JNK and MAPK signaling pathways [19]. However, the role of LINC01088 in ESCC has not been reported, and its underlying molecular mechanisms remain to be elucidated.

In the present study, we screened and characterized LINC01088 as a new target of ESCC, which is associated with tumorigenesis and metastasis. The functions of LINC01088 in ESCC were explored *in vitro* and *in vivo*. The downstream pathways were further investigated to determine its role in ESCC progression.

Materials and Methods

Bioinformatics analysis

The datasets (GSE106185, GSE17351, GSE67508, GSE21293, and GSE42363) analyzed during the current study are available in the GEO repository. A computational pipeline was established to reannotate several million probes of the Affymetrix Human Genome U133 plus 2.0 array (Supplementary Figure S1). To further increase accuracy, we adjusted a P value of less than 0.01 and $\log_2$ fold change of more than 1.5 as a threshold.

RNA-seq and GO enrichment analysis

According to the sequencing requirements of BGI (Beijing Genomics institution Company, Shenzhen, China), we prepared qualified stable cell line EC9706 that overexpressed LINC01088. The company was responsible for sequencing details, and the corresponding sequencing results were presented in the form of volcano map. GO enrichment were carried out for downregulated and upregulated genes using R package cluster Profiler. We used R package ggplot2 to visualize the important projects of each group function and pathway enrichment analysis.

Clinical specimens

Primary ESCC specimens ($n = 134$, containing matched adjacent normal tissues) were obtained from patients who underwent surgery at Peking University Cancer Hospital from 2012 to 2015. The following inclusion/exclusion criteria were applied for patients: (i) with pathological diagnosis of ESCC; (ii) with follow-up information; (iii) without preoperative chemotherapy; and (iv) without other major esophageal and tumor diseases. The detailed clinicopathological features of these patients are shown in Table 1. This study was approved by the Research and Ethical Committee of Peking University Cancer Hospital (No. 2017KT79), and it was conducted according to the principles expressed in the Declaration of Helsinki. Written informed consent was obtained from all subjects involved in the study before collection of specimens.

Table 1. Correlation between LINC01088 expression and clinicopathological parameters of patients with ESCC

Clinical parameters	Characteristics	Low (No)	High (No)	P value
Gender	Male	57	55	0.939
	Female	11	11	
Age (year)	≥9	35	27	0.375
	<60	33	39	
Section (position)	Up	22	21	0.377
	Middle	34	33	
	Low	12	12	
Living state	Survive	36	33	0.667
	Demise	31	7	
Differentiation degree	High	15	7	0.190
	Middle	41	44	
	Low	12	15	
TNM stage	I	6	9	0.576
	II	22	18	
	III	37	38	
	IV	3	1	
Lymphatic metastasis	Yes (N1,N2,N3)	41	36	0.501
	No (N0)	27	30	
Vascular tumor emboli	Yes	26	16	0.040
	No	42	50	

Cell lines and cell culture

Human ESCC cell lines (KYSE30, KYSE150, KYSE180, KYSE450, EC9706 and EC109) were purchased from the Institute of Biochemistry and Cell Biology of the Chinese Academy of Sciences (Shanghai, China). In a humidified incubator, the cells were cultured in RPMI-1640 medium (Gibco, Grand Island, USA) at 37°C with 5% CO_2. The culture medium was supplemented with 10% fetal bovine serum, 100 U/mL penicillin, and 100 μg/mL streptomycin (Gibco).

RNA interference and lentivirus shRNA vector for *LINC01088* knockdown

Small interfering RNAs (siRNAs) targeting NPM1 were customized by Genepharma (Shanghai, China). The cells were transfected with siRNA for transient knockdown using Lipofectamine 2000 (Invitrogen, Carlsbad, USA). Three short hairpin RNAs (shRNAs) targeting LINC01088 were designed and cloned into the pLenti6 vector (Genepharma) with the *U6* promoter for stable knockdown. The siRNA and shRNA sequences are listed in Table 2. The shuttle vectors containing the shRNAs were then transfected into HEK293T cells with packaging vectors using Lipofectamine 2000 (Invitrogen). The infectious lentiviruses were harvested 72 h after transfection and filtered through a 0.45-μm filter. KYSE150 or KYSE450 cells were infected with lentiviruses, followed by two weeks of selection with blasticidin (Thermo Fisher, Waltham, USA). The expression of LINC01088 in the infected cells was validated by real-time polymerase chain reaction (RT-qPCR).

Overexpression vector construction

EC9706 cells were transfected with the pCDNA3.1-LINC01088 overexpression plasmids or empty vector (as a negative control) using Lipofectamine 2000 (Invitrogen), followed by two weeks of selection with G418 (Geneticin; Invitrogen) to establish the EC9706 cell line stably expressing LINC01088.

Cell viability assay

Tumor cells were seeded in 96-well plates at a density of 3×10^3 cells/well. The number of viable cells was assessed by optical density examined at 450 nm using a CCK8 assay (Dojindo, Kumamoto, Japan) at 0, 12, 24 and 48 h according to the manufacturer's instructions.

Colony formation assay

A total of 500 cells/well were plated in 6-well plates and cultured for

Table 2. The sequences of shRNAs and siRNAs used in this study

Sample	Sequence
INC01088-shNC	Sense: 5′-GATCCACTACCGTTGTTATAGGTGCTCGAGCACCTATAACAACGGTAGTTTTTTG-3′
	Antisense: 5′-AATTCAAAAAACTACCGTTGTTATAGGTGCTCGAGCACCTATAACAACGGTAGTG-3′
LINC01088-sh37	Sense: 5′-GATCCGGATCTCTCTCTCTCAGATTTCTCGAGAAATCTGTGAAGAGAGAGAGATCCTTTTTG-3′
	Antisense: 5′-AATTCAAAAAGGATCTCTCTCTCTCAGATTTCTCGAGAAATCTGTGAAGAGAGAGAGATCCG-3′
LINC01088-sh101	Sense: 5′-GATCCGGTGAAGACCTGTGGTAAAGTCTCGAGACTTTACCACAGGTCTTCACCTTTTTG-3′
	Antisense: 5′-AATTCAAAAAGGTGAAGACCTGTGGTAAAGTCTCGAGACTTTACCACAGGTCTTCACCG-3′
LINC01088-sh122	Sense: 5′-GATCCGCTGGCAGAGAGGAAGCTAAACTCGAGTTTAGCTTCCTCTCTGCCAGCTTTTTG-3′
	Antisense: 5′-AATTCAAAAAGCTGGCAGAGAGGAAGCTAAACTCGAGTTTAGCTTCCTCTCTGCCAGCG-3′
LINC01088-sh164	Sense: 5′-GATCCGCTCAGCGTTTCACAGCTAAGCTCGAGCTTAGCTGTGAAACGCTGAGCTTTTTG-3′
	Antisense: 5′-AATTCAAAAAGCTCAGCGTTTCACAGCTAAGCTCGAGCTTAGCTGTGAAACGCTGAGCG-3′
siNPM1-NC	Sense: 5′-UUCUCCGAACGUGUCACGUTT-3′
	Antisense: 5′-ACGUGACACGUUCGGAGAATT-3′
siNPM1-1	Sense: 5′-GGAUGAGUUGCACAUUGUUTT-3′
	Antisense: 5′-AACAAUGUGCAACUCAUCCTT-3′
siNPM1-2	Sense: 5′-GGAAGCCAAAUUCAUCAAUTT-3′
	Antisense: 5′-AUUGAUGAAUUUGGCUUCCTT-3′
siNPM1-3	Sense: 5′-GGAAUGUUAUGAUAGGACATT-3′
	Antisense: 5′-UGUCCUAUCAUAACAUUCCTT-3′

2 weeks. The number of cell colonies was counted after fixed with 4% formalin and stained with 1% crystal violet.

Wound healing assay

To image the same position every time, we marked the six-well plates with six straight lines in advance. Cells were seeded into 6-well plates and scratched with a 20 μL pipette tip. After washing three times with PBS, the culture medium was changed to RPMI 1640 medium without FBS to eliminate the effects of proliferation. Detached cells were removed carefully with PBS wash for three times and the wounded area was photographed at 0, 12, 24 and 48 h (Leica, Wetzlar, Germany).

Transwell assay

Transwell insert chamber plates were used for migration and invasion assays. Transfected cells ($1–3 \times 10^5$) in 200 μL of RPMI 1640 medium supplemented with 1% FBS was added to the upper chamber and incubated at 37°C for 20 h. The lower chamber was filled with 1 mL RPMI 1640 medium supplemented with 10% FBS, and the upper chamber was coated with 60 μL diluted Matrigel (1:10; Corning Inc., Corning, USA) for the invasion assay. Non-migratory and non-invaded cells in the upper chamber were scraped off using cotton swabs. The migratory and invading cells were fixed in 4% paraformaldehyde and stained with 0.1% crystal violet. Cells were then photographed under a microscope (100 × , magnification) in three fields randomly, and then analyzed using Image J software (National Institutes of Health, Bethesda, USA).

CRISPR/Cas9-mediated NPM1 knockout

L29161 NPM1 knockout lentivirus was purchased from Beyotime Biotechnology (Shanghai, China). It can mediate the expression of pLenti-NPM1-sgRNA, which is a plasmid that can simultaneously express Cas9, sgRNA of NPM1, and puromycin resistance gene in animal cells. KYSE150 and EC9706 cells were infected with L29161 knockout lentivirus, followed by two weeks of selection with puromycin (MedChemExpress, New Jersey, USA). The knockout expression of NPM1 in the infected cells was validated by western blot analysis.

Reverse transcription and quantitative PCR

Total RNA was extracted from ESCC tissues and cell lines using Trizol reagent (Invitrogen) based on the manufacturer's instructions and was reverse transcribed to cDNA with M-MuLV Reverse Transcriptase (BioLabs, San Diego, USA). According to the manufacturer's instructions, RT-qPCR was performed with SYBR Green qPCR mix (Toyobo, Tokyo, Japan) on the 7500 Fast Real-time PCR system (Applied Biosystems, Foster City, USA). The $2^{-\triangle\triangle Ct}$ method was used for quantification, and the fold change of target genes was normalized to that of the internal control. The primer sequences are shown in Table 2.

Coimmunoprecipitation (Co-IP)

Cells were lysed using NP-40 lysis buffer (Beyotime, Shanghai, China) supplemented with 0.5% Triton X-100 (T8200; Solarbio Life Sciences, Beijing, China), RNase inhibitor (RNasin; Solarbio Life Sciences), a protease inhibitor, and phosphatase inhibitors (complete, EDTA-free; Roche Applied Science, Basel, Switzerland). The total protein concentration was determined with a BCA protein assay kit (Tiangen, Beijing, China). After normalization of the protein concentrations, lysates were immunoprecipitated with specific antibodies (anti-NPM1; ab10530; Abcam, Cambridge, UK; anti-HDM2, a mix of sc-965 and SMP-14; Santa Cruz Biotech, Santa Cruz, USA; anti-p53; ab32389; Abcam) at 4°C overnight. The immunocomplexes were collected using Protein G Sepharose beads (101241; Thermo Fisher) after 2 h of incubation. The cell lysates or immunocomplexes were separated by 10% or 12% sodium dodecyl sulfate-polyacrylamide gel electrophoresis (SDS-PAGE) and transferred to a polyvinylidene fluoride (PVDF) membrane (Millipore, Bedford, USA). Immunoblotting was carried out using the above

antibodies, followed by incubation with horseradish peroxidase (HRP)-conjugated secondary antibodies, after which the proteins were detected with enhanced chemiluminescence reagent (ECL; Pierce, Rockford, USA).

Western blot analysis

Protein samples from tissues or cells were acquired using RIPA lysis buffer (Biosharp, Hefei, China) and separated by 10% or 12% SDS-PAGE, followed by electrotransfer onto PVDF membranes. The membranes were blocked with 5% nonfat milk for 1 h, and then incubated with primary antibodies against NPM1, HDM2 (sc-965), ARF (ab185620; Abcam), p53, γH2AX (9718T; Cell Signaling Technology, Danvers, USA), p21 (12D1; Cell Signaling Technology) and GAPDH (ab8245; Abcam) overnight at 4°C. After extensive wash, membranes were incubated with the corresponding HRP-conjugated secondary antibodies. The protein bands were visualized using ECL substrate and signal intensities were measured by ImageJ software. GAPDH was used as the loading reference.

Subcellular fractionation assay

To determine the subcellular localization of LINC01088, the Cytoplasm & Nuclear RNA Purification kit (Norgen Biotek, Thorold, Canada) was used to separate the cytoplasmic and nuclear fractions according to the manufacturer's protocol. After RNA extraction, RT-qPCR was performed using SYBR Green qPCR mix (Toyobo). *GAPDH* was used as an internal reference for the cytoplasm, and *U6* was used as an internal reference for the nucleus. The sequences of the primers are shown in Table 3.

RNA pull-down and liquid chromatography-mass spectrometry (LC-MS)

KYSE150 or HEK293T cells treated with pCDNA3.1-*LINC01088*-6xMS2bs or pCDNA3.1-6xMS2bs were cotransfected with pCDNA3.1-Flag-2xMS2. The cells were collected and washed twice with PBS 48 h after transfection. Then, the cells were lysed in NP40 lysis buffer supplemented with RNase inhibitor (EO0381; Solarbio Life Sciences), a protease inhibitor, and phosphatase inhibitors (complete, EDTA-free; Roche Applied Science) at 4°C for 30 min. Finally, the cell lysates were incubated overnight with Protein G Sepharose beads bound with anti-flag antibody (Merck, Darmstadt, Germany). After the beads were washed several times, the retrieved proteins were sent to the Core Facility of Molecular Biology of Peking University Health Science Center (Beijing, China) for mass spectrometry analysis. The candidate target protein was further confirmed by western blot analysis.

Table 3. Sequences of primers used in the study

Gene	Sequence
U6	Forward: 5′-CTCGCTTCGGCAGCACA-3′
	Reverse: 5′-AACGCTTCACGAATTTGCGT-3′
LINC01088	Forward: 5′-TATTACCACAAGGCCGGCAA-3′
	Reverse: 5′-GGGCTTAGCTGTAAGGACGAA-3′
GAPDH	Forward: 5′-GGAGCGAGATCCCTCCAAAAT-3′
	Reverse: 5′-GGGCTTAGCTGTAAGGACGAA-3′
p53	Forward: 5′-CAGCACATGACGGAGGTTGT-3′
	Reverse: 5′-TCATCCAAATACTCCACACGC-3′
p21	Forward: 5′-TTAGCAGCGGAACAAGGAGT-3′
	Reverse: 5′-GCCGAGAGAAAACAGTCCAG-3′

RNA immunoprecipitation assay

HEK293T and KYSE150 cells were treated with formaldehyde to cross-link *in vivo* protein-RNA complexes. Then, the cells were washed with cold PBS and lysed with RIP buffer at 4°C for 30 min. The cell lysates were incubated overnight with Protein G Sepharose beads (101241; Thermo Fisher) conjugated to antibodies against NPM1 (Ab10530; Abcam) or normal mouse immunoglobulin G (A7028; Beyotime). After the beads were washed several times, the RNA was purified, reverse transcribed into cDNA and detected by qPCR to quantify the binding targets.

Immunofluorescence microscopy

The cells were fixed with 4% paraformaldehyde in PBS (pH 7.4) for 15 min, followed by permeabilization with 0.5% Triton X-100 for 20 min. Then, the cells were incubated with diluted primary antibody (NPM1, freshly diluted at a ratio of 1:500), placed in a wet box, and incubated at 4°C overnight. After hybridization, m-IgGk BP-CFL 488 (sc-516176; Santa Cruz) were sequentially added to visualize the signal with an inverted microscope (Leica DMi8; Leica, Darmstadt, Germany) or Zeiss LSM780 confocal microscope (Zeiss, Darmstadt, Germany). The nuclei were counterstained with 4′,6-diamidino-2-phenylindole (DAPI).

Fluorescence *in situ* hybridization (FISH) and immunohistochemistry (IHC)

A FISH assay was carried out using the LINC01088 fluorescence *in situ* hybridization kit (Boster Biological Technology, Wuhan, China) according to the supplier's instructions. After being fixed with 4% formaldehyde and washed with PBS, the KYSE150, KYSE450, and EC9706 cells or frozen sections from ESCC tumor tissue were treated with pepsin and fixed again with 1% formaldehyde. Next, the slides were incubated in prehybridization buffer at 40°C for 2–4 h. Then, the prehybridization buffer was carefully washed off with 2× SSC, 0.5× SSC, and 2× SSC for 5 min. The cells were incubated with denatured digoxin (DIG)-labelled FISH probes in hybridization buffer (50% formamide in 2× SSC) overnight at 40°C. After hybridization, anti-DIG primary antibody and fluorescein (FITC) IgG Fraction Monoclonal Mouse Anti-Biotin (AB_2339020; Jackson ImmunoResearch Labs, UK) were sequentially added to visualize the signal with an inverted microscope (Leica DMi8; Leica) or Zeiss LSM780 confocal microscope (Zeiss). The nuclei were counterstained with DAPI. For the frozen tissue sections, anti-DIG antibody labelled with biotin, streptavidin-biotin complex (SABC), and peroxidase labelled with biotin (all from Boster Biological Technology) were sequentially added. The signals were then visualized with DAB substrate. Finally, the results were evaluated by two experienced pathologists from Peking University Cancer Hospital.

Ultraviolet irradiation

In the preexperiment, 1200 J/m^2 was determined as the appropriate dose. Therefore DNA damage was induced by ultraviolet (UV) irradiation at a dose of 1200 J/m^2 using a Hoefer UVC500 Ultraviolet Crosslinker (Hoefer, San Francisco, USA). The cells were harvested, washed, and lysed with RIPA 3 h after exposure to UV irradiation. DNA damage-related proteins, such as γH2AX, were detected by western blot analysis.

Flow cytometry

An Annexin V-FITC/PI staining experiment was conducted to evaluate the proportion of EC9706 and EC9706-Lnc cells undergoing apoptosis using the flow cytometric methods. Briefly, cells were seeded into a 6-well plate (1×10^5 cells/mL) and then exposed to cisplatin (0, 4, 8, 16, and 32 μM) for 24 h. The harvested cells were centrifuged at 300 *g* for 3 min. Cells were suspended in binding buffer at 1×10^6 cells/mL. Then, 5 μL Annexin V-FITC and 5 μL PI were added and incubated in the dark for 15 min. The cell apoptotic rate was analysed using a flow cytometer (Becton Dickinson, Franklin Lakes, USA). Each assay was repeated three times.

In vivo model

A chicken chorioallantoic membrane (CAM) model was established to engraft tumor cells and monitor tumor growth and metastasis [20]. The digested KYSE150 and EC9706 cells were suspended in RPMI-1640 medium at 1×10^7 cells/mL and labelled with Cell Tracker CM-Dil (Invitrogen), which is nontoxic to cells and has prolonged stability. A hole of 3 mm in diameter was created on the eggshell with a sterile tweezer. After tumor cell engraftment, the hole was covered with a laboratory wrapping film to prevent dehydration and possible infections. The eggs were then returned to the incubator with a relative air humidity of 65% and a temperature of 37°C in a static position. After 10 days of incubation, the volume and weight of the tumor and the number of metastatic foci in the lungs in each group were evaluated.

Statistical analysis

Each experiment was repeated three times. All data are presented as the mean ± standard deviation (SD). SPSS 25.0 (SPSS Inc., Chicago, USA) or GraphPad PRISM 7 (GraphPad, San Diego, USA) was used for statistical analysis. Kaplan-Meier analysis was used to estimate the overall survival (OS) of patients with ESCC. Differences between groups were analyzed using Student's *t* test or one-way ANOVA. Differences were considered to be significant when $P < 0.05$.

Results

LINC01088 predicts a poor clinical outcome for ESCC patients

To identify the differentially expressed lncRNAs between ESCC and adjacent tissue samples (GSE106185 and GSE17351), between invasive and noninvasive EC (GSE67508 and GSE21293), and between N-positive and negative tissue samples (GSE42363) [21–24], a computational pipeline was established to reannotate several million probes of the Affymetrix Human Genome U133 plus 2.0 array (Supplementary Figure S1). To further increase accuracy, we adjusted a *P* value of less than 0.01 and $\log_2$ fold change of more than 1.5 as a threshold. Then, by intersecting the three groups, 9 downregulated lncRNAs (FLG-AS1, EIF3J-AS1, NEAT1 SPRR2C, TTTY14, SH3PXD2A-AS1, LINC01088, LOC440434 and C5orf66-AS1) and 4 upregulated lncRNAs (LOC100507053, LINC00622, MIR18A2HG and LOC642852) were identified (Figure 1A). The identified lncRNAs were confirmed to be down- or upregulated in ESCC cancer tissues by the GEPIA database. Compared with 286 normal esophageal tissues, the expression of 6 lncRNAs was decreased in 182 esophageal tumor tissues (Figure 1B). Considering the relationship between lncRNA expression and overall survival (OS) or disease-free survival (DFS) in GEPIA, 5 lncRNAs (LINC01088, C5orf66-AS1, SPRR2C, TTTY14 and SH3PXD2A-AS1) were selected as candidates (Supplementary Figure S2).

Using our cohort of 134 clinical cases collected by Peking University Cancer Hospital, we found that compared with normal adjacent tissues ESCC tissues showed downregulated expression of LINC01088 ($P = 0.0023$; Figure 1C). The expression of SH3PXD2A-AS1 was upregulated, which was not consistent with the above results. We also detected the expression of LINC01088 by immunohistochemistry, and the results suggested that LINC01088 localizes to the nucleus (Supplementary Figure S3A). To facilitate analysis, the median expression level was used as a cut-off point to classify 134 patients into the high-expression ($n = 67$) and low-expression groups ($n = 67$). Kaplan-Meier analysis was used to evaluate the predicted value of LINC01088 for survival. Compared with the patients in the high-expression group, the patients in the low-expression group showed not only a shorter survival time ($P = 0.0374$; Figure 1D) but also a higher rate of vascular tumor emboli incidence ($P = 0.040$; Table 1). The patients with vascular tumor emboli in the low-expression group had a significant reduction in overall survival time (Figure 1E).

LINC01088 suppresses the malignant phenotype of ESCC cells

The KYSE150 and KYSE450 cell lines have a relatively higher expression of LINC01088, so these cell lines were utilized for knockdown experiments. The EC9706 and KYSE180 cell lines were utilized for the overexpression experiments (Supplementary Figure S2B). Stable EC9706 and KYSE180 cell lines overexpressing LINC01088 and stable KYSE150 and KYSE450 cell lines in which *LINC01088* was knocked down were constructed and validated (Figure 2A and Supplementary Figure S2C). The CCK-8 assay showed that the proliferation ability was decreased in the EC9706 and KYSE180 cell lines overexpressing LINC01088, while the proliferation ability was increased in the KYSE150 and KYSE450 cell lines with *LINC01088* knockdown (Figure 2B and Supplementary Figure S2D). Furthermore, LINC01088 overexpression markedly decreased colony formation, while knockdown of *LINC01088* increased colony formation (Figure 2C and Supplementary Figure S2E,F). Next, we examined the effect of LINC01088 on cell migration and invasion via wound healing and Transwell assays. Knockdown of *LINC01088* led to a significant increase in the migration and invasion ability of the KYSE150 and KYSE450 cell lines, whereas LINC01088 overexpression inhibited the migration and invasion ability of the EC9706 and KYSE180 cell lines (Figure 2D,E and Supplementary Figure S2G,H). We also established the chicken chorioallantois membrane model (CAM), which displays tumor growth and spontaneous metastatic events. The digested tumor cells were labelled with Cell Tracker CM-Dil. The results showed that the tumor volume and weight and the number of metastatic foci in the lungs in the knockdown group were increased, and the LINC01088 overexpression group showed the opposite results (Figure 2F,G). Collectively, these results indicate that LINC01088 can negatively affect ESCC cell proliferation, migration and invasion both *in vivo* and *in vitro*.

NPM1 is a target of LINC01088

Next, we explored the underlying antitumor mechanisms of LINC01088. According to the cellular fractionation results, LINC01088 was primarily found in the nucleus of ESCC cells (Figure 3A). This result was consistent with the immunohistochemical results

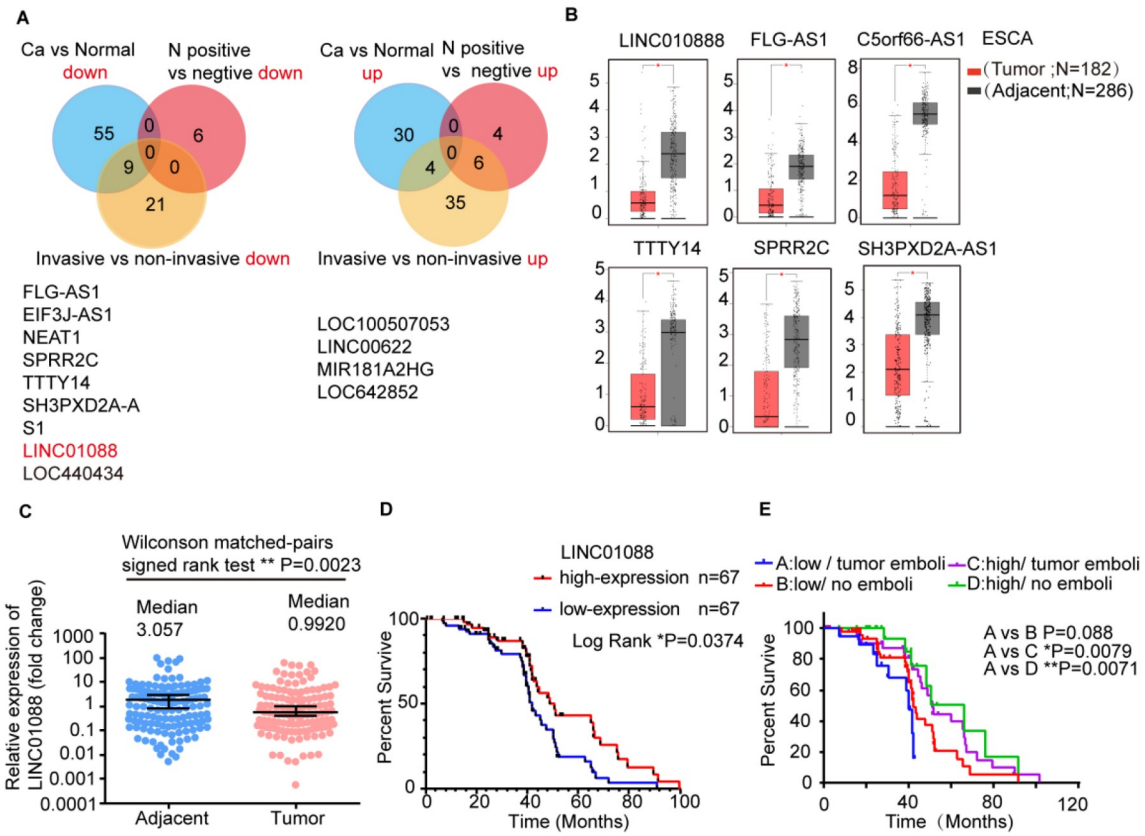

Figure 1. Increased LINC01088 expression is related to a favorable prognosis in ESCC patients (A) A Venn diagram of three independent lncRNA differential analyses. Blue: between tumor and adjacent tissue samples; Green: between invasive and noninvasive EC samples; Red: between N-positive and N-negative EC samples. (B) The expression levels of 6 lncRNAs in 286 normal tissues and 182 ESCC tumor tissues based on data from the GEPIA database. (C) The expression levels of LINC01088 in a cohort of 134 ESCC tumor tissues and paired adjacent tissues collected by Peking University Cancer Hospital. (D) Kaplan-Meier curves of the LINC01088 high-expression and low-expression groups for overall survival time (OS). (E) The patients with vascular tumor emboli in the low-expression group had a significant reduction in OS time. Data are shown as the mean ± SD. $*P<0.05$, $**P<0.01$.

(Supplementary Figure S2A) and FISH assay results in which LINC01088 was labelled with fluorescence (Figure 3B). LINC01088 may regulate gene transcription and translation by directly binding to proteins, transcription factors or DNA [25]. To determine the potential interaction targets, RNA pull-down and LC-MS were performed (Figure 3C,D). HSPD1, nucleophosmin (NPM1) and PCNA were among the top candidates. Next, the existence of NPM1 was validated by western blot analysis (Figure 3E), and the results for other candidate proteins were negative. We consistently verified this interaction via RIP assays and observed the enrichment of LINC01088 in the NPM1 group (Figure 3F). Finally, we identified the interaction *in vivo*. We also applied RNA-seq to the stably overexpressed cell lines (Supplementary Figure S4A), and found that the expression of NPM1 did not change significantly (Supplementary Figure S4B). This finding indicates that LINC01088 may not change the expression or protein stability of NPM1. The GO enrichment analysis results confirmed that the transcription factor and transcriptional activator activity were closely related pathways (Supplementary Figure S3C). The expressions of oncogenes, such as c-Myc, TERT and HNF1A, were reduced, further confirming the antitumor effect of LINC01088 (Supplementary Figure S3B). HNF1A and c-Myc expression levels were verified by western blot analysis (data not shown).

The inhibition of ESCC progression by LINC01088 is dependent on NPM1

To determine whether the inhibition of ESCC progression by LINC01088 is dependent on NPM1, we knocked out *NPM1* in EC9706 cells overexpressing LINC01088 (EC9706-Lnc). CRISPR/Cas9-mediated *NPM1* knockout led to rapid ESCC death, and we speculated that the normal physiological function of NPM1 was disrupted. Two different siRNAs were confirmed to knockdown *NPM1* expression in EC9706 cells by RT-qPCR analysis (Figure 4A). We found that the viability of EC9706-Lnc cells was increased (Figure 4B) when NPM1 was downregulated. Similar results were also observed in the cytofunctional experiments. Knockdown of *NPM1* promoted migration and invasion of LINC01088-overexpressing EC9706 cells (Figure 4C,D). All these results indicate that the ability of LINC01088 to inhibit ESCC proliferation, invasion and metastasis is dependent on NPM1.

LINC01088 regulates mut-p53 by influencing the translocation of NPM1 and its interaction with HDM2

NPM1 is a widely expressed nucleolar phosphoprotein that constantly shuttles between the nucleus and cytoplasm [26,27]. Dysregulation of NPM1 expression and localization contributes to tumorigenesis through different mechanisms [26,28–30]. The

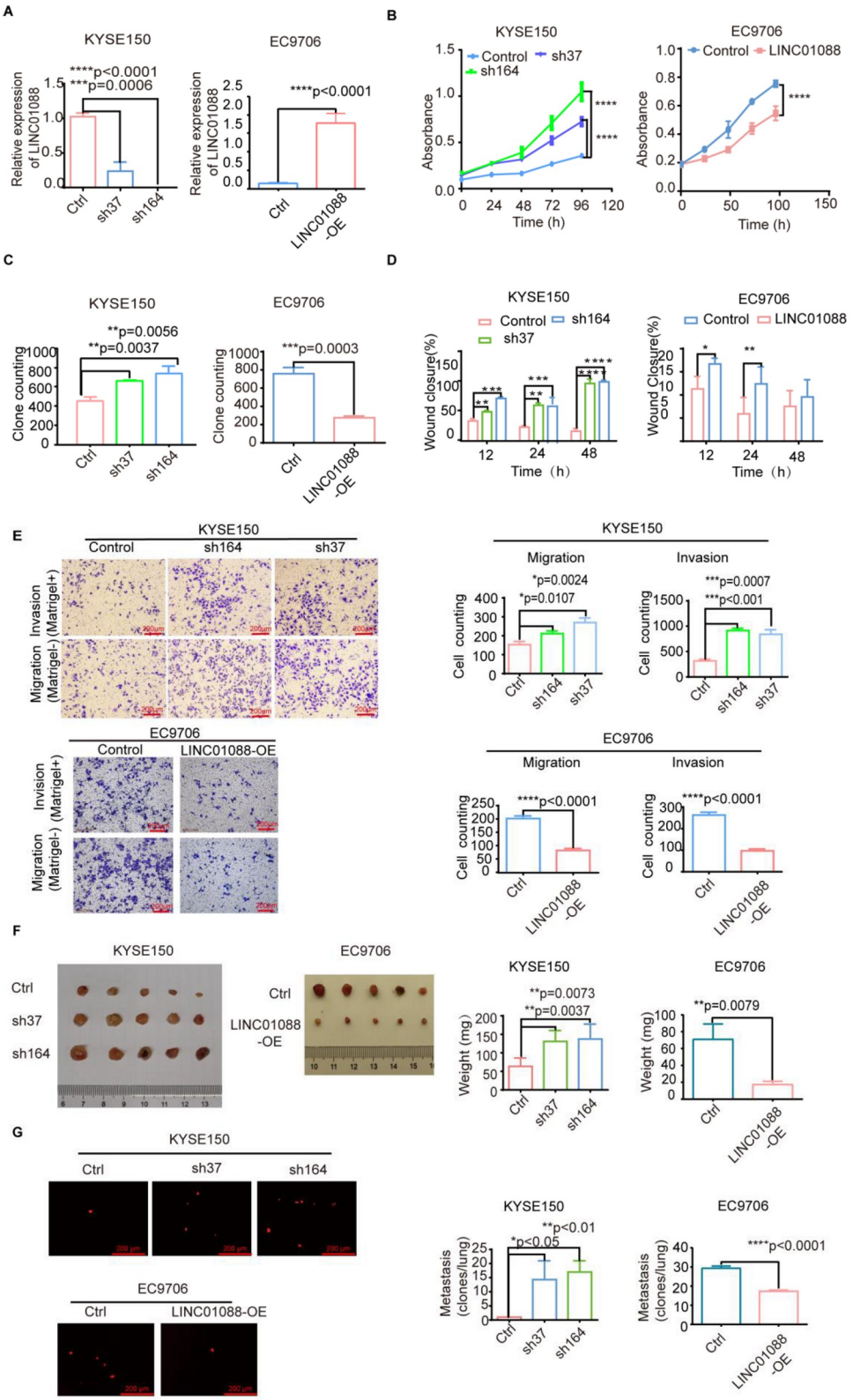

Figure 2. LINC01088 expression negatively affects the ESCC cell malignant phenotype (A) The stable cell lines overexpressing LINC01088 and those with knockdown of *LINC01088* were validated by RT-qPCR analysis, and sh37 and sh164 were the effective interference targets. (B) CCK8 assays showed that the proliferation ability was inhibited by LINC01088. (C) Colony formation assays showed that the colony formation ability was negatively correlated with LINC01088 expression. (D) Wound healing assay showed LINC01088 inhibited the migration ability. (E) Transwell assays showed that LINC01088 inhibited cell migration and invasion abilities. (F,G) In the CAM model, tumor volume and weight and metastatic foci were decreased after LINC01088 overexpression. Data are shown as the mean ± SD. *$P < 0.05$, **$P < 0.01$, ***$P < 0.001$, ****$P < 0.0001$.

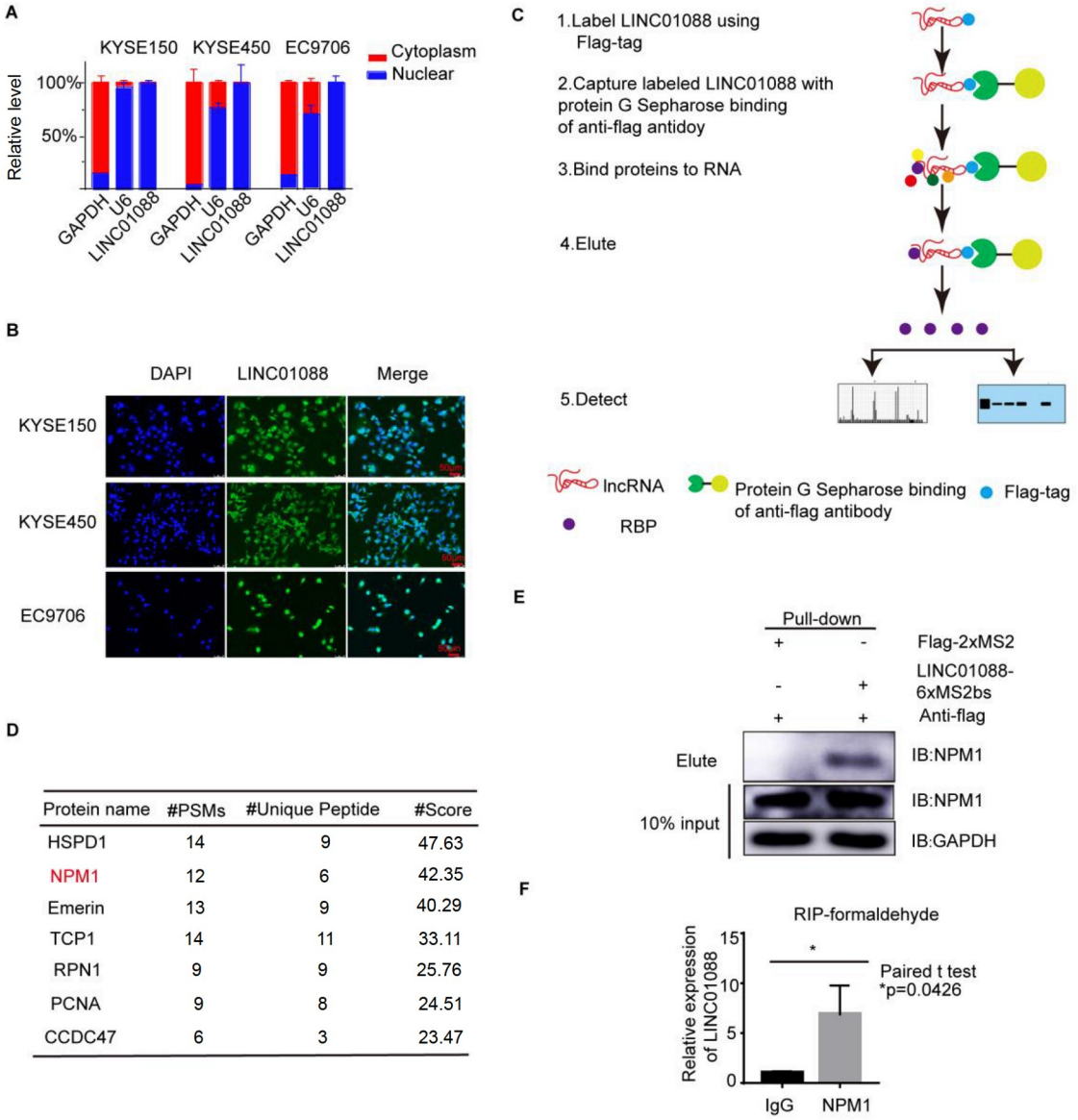

Figure 3. NPM1 is a target of LINC01088 (A) Intracellular localization of LINC01088 was assessed by RT-qPCR. *U6* and *GAPDH* were the preference controls for nuclear RNA and cytoplasmic RNA, respectively. (B) FISH assay showed that LINC01088 was mainly expressed in the nucleus. DAPI staining shows the nucleus. Scale bar: 5 μm. (C) 293T cell lysates were incubated overnight with protein G Sepharose binding of anti-flag antibody for RNA pull-down assay and mass spectrometry (MS). (D) The top candidates obtained by LC-MS analysis are listed. (E) 293T cell lysates were immunoprecipitated with anti-NPM1 antibody or IgG control. (F) RIP-PCR was applied to determine the amount of LINC01088 associated with NPM1 immunoprecipitation relative to the IgG control. Data are shown as the mean ± SD. *$P < 0.05$.

GEPIA database indicated that there is no significant correlation between NPM1 expression and LINC01088 expression (data not shown). Therefore, we suspected that LINC01088 may affect the localization of NPM1. Confocal laser scanning microscopy results showed that the expression ratio of NPM1 in the cytoplasm and nucleoplasm versus the nucleolus in ESCC was changed with LINC01088 overexpression (Figure 5A). Compared with that in the EC9706-Ctrl group, the number of positive cells with a ratio change was significantly increased in the EC9706-Lnc group ($P = 0.008$; Figure 5A).Based on data from the STRING database (https://string-db.org/.), a highly interconnected protein network, NPM1-HDM2-p53, was identified (Figure 5B). NPM1 is closely associated with tumor protein p53 (TP53 or p53) [25,29,31]. It directly interacts with p53 and regulates the increase in stability and transcription activity. The ubiquitin-proteasome system plays a role in ESCC, and ubiquitin protein ligase can regulate a number of tumor-associated proteins via ubiquitination. NPM1 could influence p53 degradation by interacting with the human double minute 2 protein (HDM2) [29,32,33]. NPM1 also has an inhibitory effect on the expression of HDM2 to regulate mut-p53 stability in tumors [31,34].

TP53 is by far the most frequently mutated gene in ESCC [35,36], and over 80% of mutant p53 proteins (mut-p53) have acquired gain-of-function (GOF) activities [37,38].These activities enable them to both inactivate wild-type p53 (wt-p53) and promote tumor progression. The ESCC cell lines in this study are all p53-mutant cell lines [39–42]. Under stressful conditions, transient expression of the

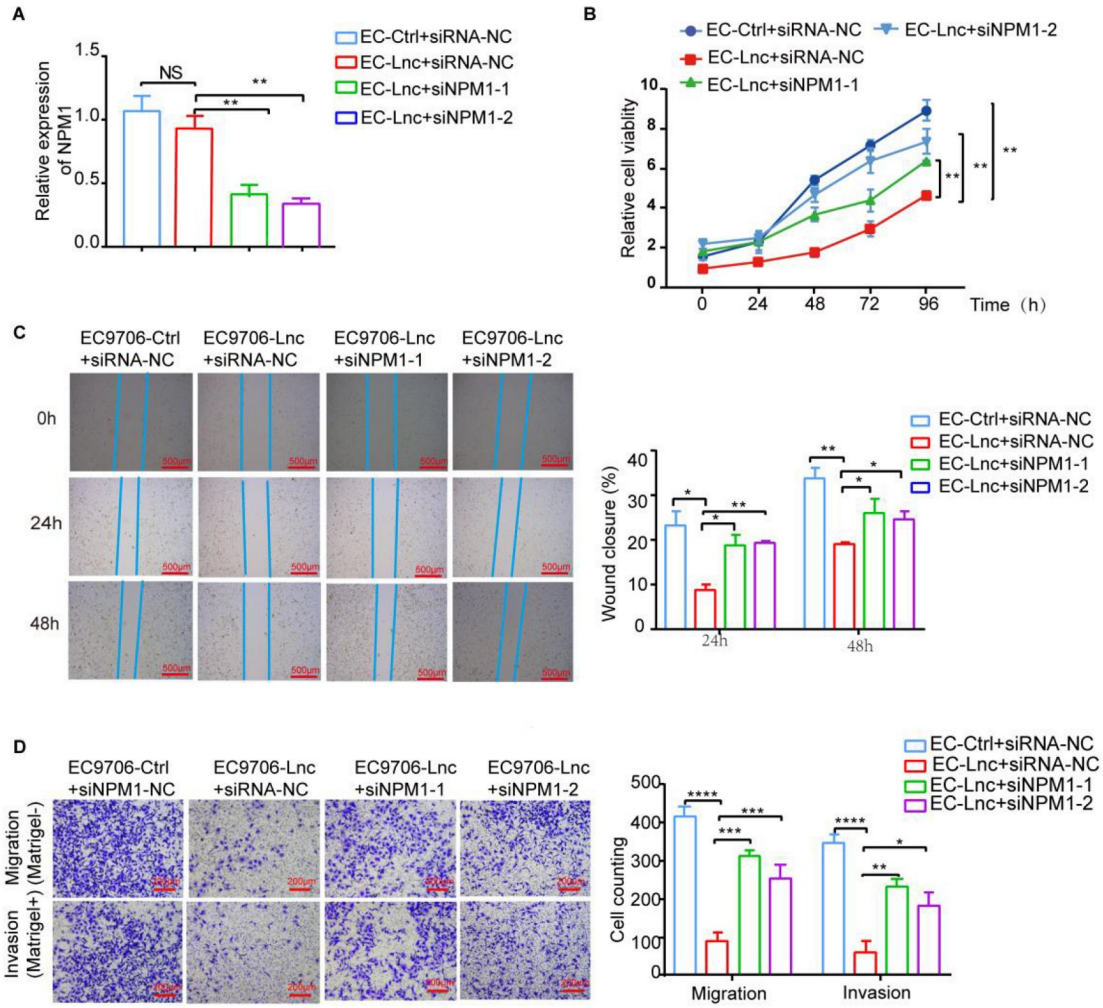

Figure 4. Inhibition of ESCC progression by LINC01088 is dependent on NPM1 (A) Knockdown of *NPM1* in EC9706 cells overexpressing LINC01088 (EC-Lnc) was confirmed by RT-qPCR analysis. (B) CCK8 assays showed that the viability of EC-Lnc cells was increased after *NPM1* knockdown. (C,D) Wound healing and Transwell assays showed that the ability of LINC01088 to inhibit ESCC migration and invasion was attenuated when *NPM1* was knocked down. Scale bar: 500 μm in C and 200 μm in D. Data are shown as the mean ± SD. $*P<0.05$, $**P<0.01$, $***P<0.001$, $****P<0.0001$.

cyclin-dependent kinase inhibitor (CKI) p21 is promoted in a p53-dependent manner [43]. However, the normal function of the p53 pathway is ubiquitously lost in cancers either through mutation or inactivating interactions [44].

We speculated that LINC01088 may affect mut-p53 expression by affecting the binding of NPM1 to p53, HDM2 or ARF. The Co-IP assay revealed that NPM1 interacted with HDM2, but p53 and ARF were not detected. Furthermore, the amount of HDM2 protein bound to NPM1 was decreased. These findings indicate that LINC01088 disrupted NPM1-HDM2 complex formation in the EC9706 cell line and increased free HDM2 in the cytoplasm and nucleoplasm (Figure 5C). The amount of NPM1 protein bound to HDM2 was also decreased in the presence of LINC01088. RT-qPCR and western blot analysis results showed that mut-p53 was decreased and p21 was increased at both the protein and mRNA levels in the presence of LINC01088. These findings suggest that the normal transcription activity of p53 was rescued (Figure 5D,E), and knockdown of *LINC01088* increased mut-p53 expression at the protein level (Figure 5E).

We also tried to predict the potential binding sites of LINC01088 in the promoter region of *p53* using the JASPAR 2020 database but were not successful. It is unlikely that LINC01088 directly regulates mut-p53 expression. Based on the above results, it is highly possible that LINC01088 regulates the expression of mut-p53 by affecting the binding of NPM1 to HDM2. Increased level of free HDM2 protein in the nucleoplasm leads to the degradation of mut-p53 protein.

LINC01088 may disrupt the DNA repair function of NPM1

NPM1 acts as a molecular chaperone during DNA damage repair. It not only plays a significant role in the base excision DNA repair (BER) of DNA lesions [33] but also affects translesion DNA synthesis (TLS) [39]. NPM1 SUMOylation is indispensable for the assembly of the BRCA1 complex at the early stage of the DNA-damage response (DDR) [45]. Its expression in the nucleolus is also essential for the caspase-2 activation cascade in response to a variety of forms of DNA damage [46,47]. Considering the distribution change and competitive association, we explored whether LINC01088 disturbs the DSB repair function of NPM1. γH2AX (phospho-H2A. X Variant Histone) is a sensitive marker for DSB after radiation or chemotherapy [48]. As DSBs are repaired, γH2AX

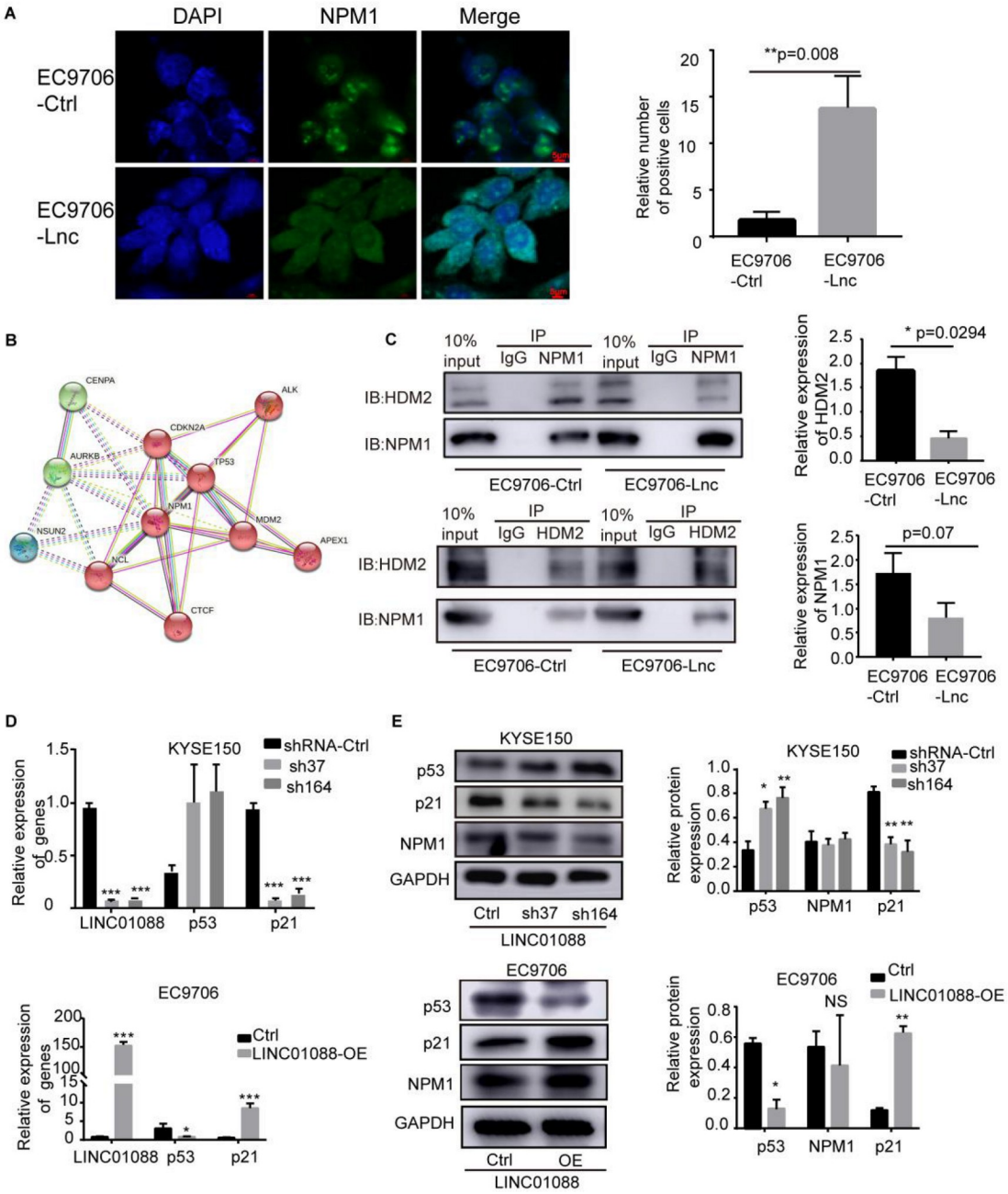

Figure 5. LINC01088 regulates mut-p53 by influencing the translocation of NPM1 and its interaction with HDM2 (A) Immunofluorescence results showed that the expression ratio of NPM1 in the nucleoplasm versus the nucleolus was changed, and the number of cells with a positive change in the EC9706-*LINC01088* group was significantly increased compared with that in the EC9706-Ctrl group. Scale bar: 5 μm. (B) The STRING database showed a highly interconnected protein network of NPM1-HDM2-p53. (C) The Co-IP assay revealed that NPM1 interacted with HDM2, and LINC01088 inhibited NPM1-HDM2 complex formation. (D) LINC01088 overexpression rescued the transcriptional activity of mut-p53, and *p21* expression was increased at the mRNA level. (E) LINC01088 overexpression inhibited mut-p53 expression and promoted p21 expression at the protein level. Data are shown as the mean ± SD. $*P<0.05$, $**P<0.01$, $***P<0.001$.

foci disappear. Under UV irradiation, γH2AX expression was decreased after *LINC01088* knockdown (Figure 6A), and this effect was rescued by concomitant knockdown of *NPM1* (Figure 6B). These findings indicate its dependence on NPM1-mediated DNA repair. Additionally, LINC01088 overexpression resulted in increased γH2AX expression (Figure 6C), but there was no difference between the control and overexpression groups in the absence of ultraviolet stimulation. Cisplatin is an antineoplastic chemotherapy agent that works by cross-linking with DNA and causing DNA damage in cancer cells [49]. The half-maximal inhibitory concentration (IC_{50}) values were measured to assess the sensitivity to cisplatin. The IC_{50} of the EC9706-LINC01088 group ($\log_2 IC_{50} = 7.911 \pm 1.128$ μM) was significantly lower than that of the EC9706-Ctrl group ($\log_2 IC_{50} = 21.87 \pm 2.98$ μM) (Figure 6D). To evaluate the effects of LINC01088 on the cisplatin-induced apoptosis of EC9706 or EC9706-Lnc cells, we performed flow cytometric analysis with

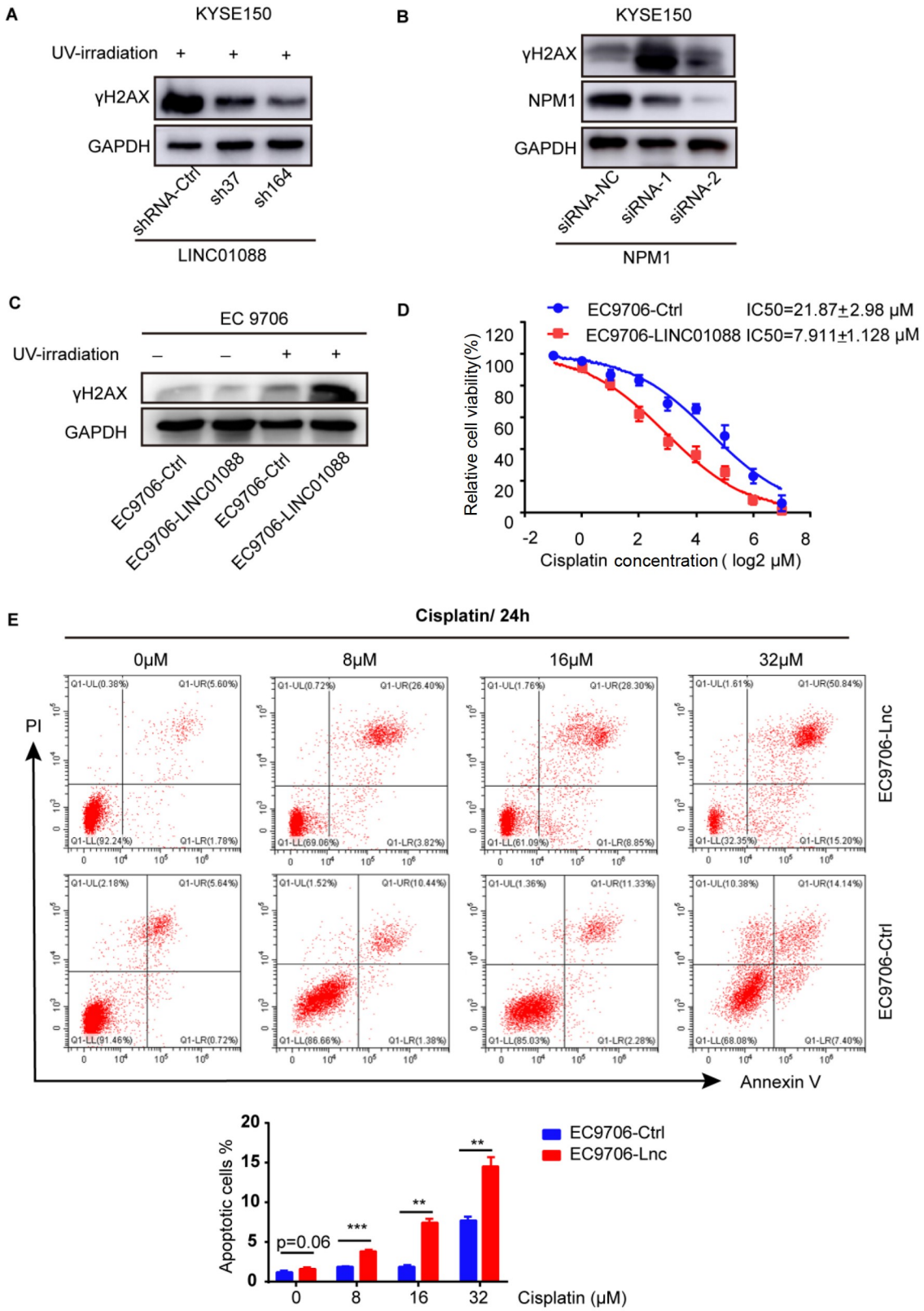

Figure 6. LINC01088 may disturb the DNA repair function of NPM1 (A) Knockdown of *LINC01088* decreased the DNA damage induced by ultraviolet irradiation, and (B) silencing of *NPM1* by siRNA rescued the result. (C) Overexpression of LINC01088 enhanced the DNA DSBs induced by ultraviolet irradiation. (D) The IC_{50} value of EC9706 to cisplatin was decreased in the presence of LINC01088. (E) Effects of LINC01088 on the cisplatin-induced apoptosis of EC9706 and EC9706-Lnc cells were evaluated by flow cytometry with Annexin V-FITC/PI dual staining. Data are shown as the mean ± SD. $^{**}P < 0.01$, $^{***}P < 0.001$.

Annexin V-FITC/PI double staining (Figure 6E). The proportion of early apoptosis (Annexin V-FITC$^+$/PI$^-$) and late apoptosis (Annexin V-FITC$^+$/PI$^+$) in the EC9706 or EC9706-Lnc group was 1.78% ± 5.60% and 0.72% ± 5.64%, respectively. After the cells were exposed to 8, 16 or 32 μM cisplatin, the percentages of early and late apoptosis were increased to 3.82% ± 26.40%, 8.85% ± 28.30% and 8.85% ± 50.84%, respectively, which were significantly higher than those of the EC9706 group (1.38% ± 10.44%, 2.28% ± 11.33% and 7.40% ± 14.14%; $P < 0.01$). Our results indicated that LINC01088 increased the sensitivity of EC9706 cells to chemotherapeutic drugs and radiotherapy. The antitumor effects of LINC01088 on ESCC may be related to the impaired DNA repair function of NPM1, at least partially.

Discussion

A few lncRNAs have been demonstrated to have clinical application value in ESCC [50–54]. The priority for future research in this area should focus on the use of lncRNAs as molecular targets in clinical diagnosis and treatment. The aim of this study was to explore differentially expressed lncRNAs associated with ESCC invasion and metastasis. We identified a novel endogenous lncRNA, LINC01088 that was downregulated in ESCC. This study showed that LINC01088 negatively affected ESCC cell proliferation, migration and invasion abilities *in vitro* and *in vivo*. Previous findings provided multiple molecular mechanisms through which LINC01088 executes protumor or antitumor function. LINC01088 could bind to different microRNAs or RNA-binding proteins. These results suggested that LINC01088 regulated cancer progression in a cell type-dependent manner and could play contradictory roles among different cancers.Here, RNA pull-down and RIP analyses suggested that LINC01088 physically interacts with NPM1. The role of NPM1 in hematological tumors has received extensive attention, but there has been little focus on NPM1 in solid tumors. Unlike the abnormal mutations in hematological tumors [55,56], NPM1 is rarely mutated and is often overexpressed in solid tumors of diverse histological origins [57–59]. Under stress and oncogenic stimuli, increased NPM1 level promotes proliferation and inhibits apoptosis. In this study, we provided experimental evidence that NPM1 plays a role in ESCC. The inhibition of ESCC progression by LINC01088 is dependent on NPM1. In the rescue assay, after *NPM1* was knocked down in LINC01088-overexpressing cells, the proliferation, migration and invasion trends were reversed. However, knockdown of *NPM1* only slightly affects the proliferation, migration and invasion of ESCC. When LINC01088 is overexpressed, the inhibitory effect on ESCC is more significant. This phenomenon may be related to the dynamic changes in the distribution of NPM1 between the nucleolus and nucleoplasm. In another study, the lncRNA LETN was concentrated in the nucleolus by directly binding to NPM1, which contributed to the formation of NPM1 oligomers [60]. The oligomerization of NPM1 has been linked to its nucleolar localization and role in cell proliferation. These findings indicate that LINC01088 promotes the nucleoplasm location of NPM1 and disturbs its proliferative capacity.

Our work also showed that LINC01088 disturbed the interaction between NPM1 and HDM2. In recent years, a large number of studies have shown that the protein-nucleic acid complex binds to and inhibits the E3 ubiquitin ligase activity of the oncogene MDM2, which ubiquitinates p53 and regulates the level of intracellular p53 protein [61–63]. It has been reported that the lncRNA SAMD12-AS1 interacts with NPM1 by promoting p53 degradation, and its association with HDM2 is impaired [64]. When LINC01088 is overexpressed, the interaction between NPM1 and HDM2 is disrupted, and mut-p53 protein level is decreased. It is highly possible that an increase in the amount of free HDM2 protein in the nucleoplasm leads to the degradation of mut-p53 protein. NPM1 also regulates apoptosis by inhibiting caspases and endonucleases or regulating tumor suppressors, including ARF and p53 [26,65,66]. It is highly likely that the mechanism by which NPM1 binds with mut-p53 to promote its stability is weakened.

TP53 mutation is significantly correlated with various biological behaviors of ESCC, such as differentiation degree, tumor invasion, and lymph node metastasis [67–70]. Detection of p53 protein mutation and expression in ESCC is helpful to determine the degree of malignancy and prognosis of patients. Increasing evidence indicates that downregulation of mut-p53 expression in cancer cells reduces their aggressive properties [71,72], restores wt-p53 activity and increases the transcripts of p53 downstream target genes [71]. To date, several lncRNAs, such as lincRNA-p21, PANDA, PINT, NEAT1, GUARDIN, and DINO, have been reported to function as downstream effectors of p53 [73–81], whereas more lncRNAs with p53 regulatory functions remain to be discovered. Our work revealed that LINC01088 is a novel lncRNA involved in regulating mut-p53 expression via the NPM1-HDM2 pathway. LINC01088 inhibits ESCC proliferation, invasion and metastasis by targeting the NPM1-HDM2-p53 axis. The interaction between HDM2 and mut-p53 needs to be explored and ubiquitination experiments need to be performed, and whether different p53 mutation types affect the antitumor function of LINC00188 remains unclear and needs further exploration.

Aberrantly localized NPM1 may also promote tumor progression by participating in DNA damage repair or rRNA synthesis. NPM1 plays vital roles in centrosome duplication, genome stability and responses to various DNA damaging or cytotoxic agents [30,82,83]. Previous studies have reported that DNA damage induces a switch in the aberrant cytoplasmic localization of NPM1 mutants back to a predominantly nucleolar localization [83], and the chemotherapeutic oxaliplatin causes cell death via the inhibition of rRNA synthesis accompanied by NPM1 relocalization [30]. Cytoplasmic-localized NPM1 mutants play a dramatic role in the development of AML [84–86]. The DNA repair process involving NPM1 occurs in the nucleoplasm. This study indicated that the DNA repair function of NPM1 was disrupted by nuclear-retained LINC01088. The sensitivity of EC9706 cells to chemotherapeutic drugs or radiotherapy was increased. NPM1 in the nucleoplasm may be a potential target of ESCC. Combined with the effect of mut-p53 on chemotherapy resistance and the DNA damage repair function of NPM1, LINC01088 may be related to the efficacy of chemotherapy drugs on ESCC, which needs further study.

Based on the above results, we proposed a model depicting the critical role of LINC01088 in ESCC (Figure 7). To the best of our knowledge, our results are the first to prove that LINC01088 suppresses ESCC cell tumorigenesis and metastasis both *in vitro* and *in vivo*. LINC01088 impairs the interaction between NPM1 and mut-p53, which is the downstream target. LINC01088 is also involved in disrupting the DNA repair function of NPM1. The exact mechanism of action involved in this process needs further research. Previous studies on NPM1 have predominantly focused on hematological tumors, and the role of NPM1 in solid tumors has only recently been

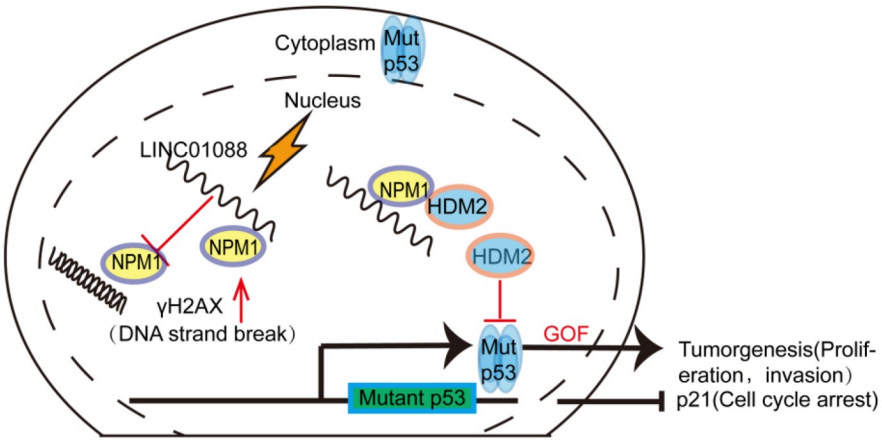

Figure 7. A schematic illustration of the proposed model depicting the role of LINC01088 in inhibiting ESCC progression

recognized. Our study indicates that NPM1 functions in ESCC and highlights the potential of LINC01088 as a prognostic biomarker and therapeutic target for ESCC.

Supplementary Data

Supplementary data is available at *Acta Biochimica et Biophysica Sinica* online.

Acknowledgement

We thank Dr. RH Yang (Beijing Institute of Hepatology, Beijing Youan Hospital, Capital Medical University, Beijing, China) and Dr. YX Zhang (Jinan Central Hospital Affiliated to Shandong First Medical University, Jinan, China) for their valuable suggestion

Funding

This work was supported by the grants from the National Natural Science Foundation of China (Nos. 81773144 and 81772632), Capital Health Development Scientific Research Project (No. SF2018-2-2155) and Science Foundation of Peking University Cancer Hospital (No. A002208). The APC was funded by Peking University Cancer Hospital.

Conflict of Interest

The authors declare that they have no conflict of interest.

References

1. Sung H, Ferlay J, Siegel RL, Laversanne M, Soerjomataram I, Jemal A, Bray F. Global cancer statistics 2020: GLOBOCAN estimates of incidence and mortality worldwide for 36 cancers in 185 countries. *CA Cancer J Clin* 2021, 71: 209–249
2. Umar SB, Fleischer DE. Esophageal cancer: epidemiology, pathogenesis and prevention. *Nat Rev Gastroenterol Hepatol* 2008, 5: 517–526
3. Lin Y, Totsuka Y, Shan B, Wang C, Wei W, Qiao Y, Kikuchi S, *et al.* Esophageal cancer in high-risk areas of China: research progress and challenges. *Ann Epidemiol* 2017, 27: 215–221
4. Morgan E, Soerjomataram I, Gavin AT, Rutherford MJ, Gatenby P, Bardot A, Ferlay J, *et al.* International trends in oesophageal cancer survival by histological subtype between 1995 and 2014. *Gut* 2020, 70: 234
5. Thrumurthy SG, Chaudry MA, Thrumurthy SSD, Mughal M. Oesophageal cancer: risks, prevention, and diagnosis. *BMJ* 2019, 366: l4373
6. Pennathur A, Gibson MK, Jobe BA, Luketich JD. Oesophageal carcinoma. *Lancet* 2013, 381: 400–412
7. Jemal A, Siegel R, Ward E, Hao Y, Xu J, Thun MJ. Cancer statistics, 2009. *CA Cancer J Clin* 2009, 59: 225–249
8. Yang J, Liu X, Cao S, Dong X, Rao S, Cai K. Understanding esophageal cancer: the challenges and opportunities for the next decade. *Front Oncol* 2020, 10: 1727
9. Goodall GJ, Wickramasinghe VO. RNA in cancer. *Nat Rev Cancer* 2021, 21: 22–36
10. Bhan A, Soleimani M, Mandal SS. Long noncoding rna and cancer: a new paradigm. *Cancer Res* 2017, 77: 3965–3981
11. Rinn JL, Chang HY. Genome regulation by long noncoding RNAs. *Annu Rev Biochem* 2012, 81: 145–166
12. Wu Y, Hu L, Liang Y, Li J, Wang K, Chen X, Meng H, *et al.* Up-regulation of lncRNA CASC9 promotes esophageal squamous cell carcinoma growth by negatively regulating PDCD4 expression through EZH2. *Mol Cancer* 2017, 16: 150
13. Wang B, Hao X, Li X, Liang Y, Li F, Yang K, Chen H, *et al.* Long noncoding RNA HEIH depletion depresses esophageal carcinoma cell progression by upregulating microRNA-185 and downregulating KLK5. *Cell Death Dis* 2020, 11: 1002
14. Chen LL. Linking Long Noncoding RNA Localization and Function. *Trends Biochem Sci* 2016, 41: 761–772
15. Ponting CP, Oliver PL, Reik W. Evolution and functions of long noncoding RNAs. *Cell* 2009, 136: 629–641
16. Zhang W, Fei J, Yu S, Shen J, Zhu X, Sadhukhan A, Lu W, *et al.* LINC01088 inhibits tumorigenesis of ovarian epithelial cells by targeting miR-24-1-5p. *Sci Rep* 2018, 8: 2876
17. Liu JQ, Feng YH, Zeng S, Zhong MZ. Linc01088 promotes cell proliferation by scaffolding EZH2 and repressing p21 in human non-small cell lung cancer. *Life Sci* 2020, 241: 117134
18. Peng T, Chen DL, Chen SL. LINC01088 promotes the growth and invasion of glioma cells through regulating small nuclear ribonucleoprotein polypeptide A transcription. *Bioengineered* 2022, 13: 9172–9183
19. Zhao H, Li Y, Dong N, Zhang L, Chen X, Mao H, Al-Ameri SAAE, *et al.* LncRNA LINC01088 inhibits the function of trophoblast cells, activates the MAPK-signaling pathway and associates with recurrent pregnancy loss. *Mol Hum Reprod* 2021, 27: gaab047
20. Nowak-Sliwinska P, Segura T, Iruela-Arispe ML. The chicken chorioallantoic membrane model in biology, medicine and bioengineering. *Angiogenesis* 2014, 17: 779–804
21. Lee JJ, Natsuizaka M, Ohashi S, Wong GS, Takaoka M, Michaylira CZ, Budo D, *et al.* Hypoxia activates the cyclooxygenase-2–prostaglandin E synthase axis. *Carcinogenesis* 2010, 31: 427–434

22. Yamakita I, Mimae T, Tsutani Y, Miyata Y, Ito A, Okada M. Guanylate binding protein 1 (GBP-1) promotes cell motility and invasiveness of lung adenocarcinoma. *Biochem Biophys Res Commun* 2019, 518: 266–272
23. Chen K, Li Y, Dai Y, Li J, Qin Y, Zhu Y, Zeng T, *et al.* Characterization of tumor suppressive function of cornulin in esophageal squamous cell carcinoma. *PLoS ONE* 2013, 8: e68838
24. Michaylira CZ, Wong GS, Miller CG, Gutierrez CM, Nakagawa H, Hammond R, Klein-Szanto AJ, *et al.* Periostin, a cell adhesion molecule, facilitates invasion in the tumor microenvironment and annotates a novel tumor-invasive signature in esophageal cancer. *Cancer Res* 2010, 70: 5281–5292
25. Bertwistle D, Sugimoto M, Sherr CJ. Physical and functional interactions of the Arf tumor suppressor protein with nucleophosmin/B23. *Mol Cell Biol* 2004, 24: 985–996
26. Colombo E, Marine JC, Danovi D, Falini B, Pelicci PG. Nucleophosmin regulates the stability and transcriptional activity of p53. *Nat Cell Biol* 2002, 4: 529–533
27. Zarka J, Short NJ, Kanagal-Shamanna R, Issa GC. Nucleophosmin 1 mutations in acute myeloid leukemia. *Genes* 2020, 11: 649
28. Wade M, Li YC, Wahl GM. MDM2, MDMX and p53 in oncogenesis and cancer therapy. *Nat Rev Cancer* 2013, 13: 83–96
29. Kurki S, Peltonen K, Latonen L, Kiviharju TM, Ojala PM, Meek D, Laiho M. Nucleolar protein NPM interacts with HDM2 and protects tumor suppressor protein p53 from HDM2-mediated degradation. *Cancer Cell* 2004, 5: 465–475
30. Sutton EC, DeRose VJ. Early nucleolar responses differentiate mechanisms of cell death induced by oxaliplatin and cisplatin. *J Biol Chem* 2021, 296: 100633
31. Ren Z, Aerts JL, Vandenplas H, Wang JA, Gorbenko O, Chen JP, Giron P, *et al.* Phosphorylated STAT5 regulates p53 expression via BRCA1/BARD1-NPM1 and MDM2. *Cell Death Dis* 2016, 7: e2560
32. Fang S, Jensen JP, Ludwig RL, Vousden KH, Weissman AM. Mdm2 is a RING finger-dependent ubiquitin protein ligase for itself and p53. *J Biol Chem* 2000, 275: 8945–8951
33. Honda R, Yasuda H. Activity of MDM2, a ubiquitin ligase, toward p53 or itself is dependent on the RING finger domain of the ligase. *Oncogene* 2000, 19: 1473–1476
34. Hamilton G, Abraham AG, Morton J, Sampson O, Pefani DE, Khoronenkova S, Grawenda A, *et al.* AKT regulates NPM dependent ARF localization and p53mut stability in tumors. *Oncotarget* 2014, 5: 6142–6167
35. Kandoth C, McLellan MD, Vandin F, Ye K, Niu B, Lu C, Xie M, *et al.* Mutational landscape and significance across 12 major cancer types. *Nature* 2013, 502: 333–339
36. Soussi T, Wiman KG. TP53: an oncogene in disguise. *Cell Death Differ* 2015, 22: 1239–1249
37. Leroy B, Anderson M, Soussi T. TP53 mutations in human cancer: database reassessment and prospects for the next decade. *Hum Mutat* 2014, 35: 672–688
38. Bouaoun L, Sonkin D, Ardin M, Hollstein M, Byrnes G, Zavadil J, Olivier M. *TP53* variations in human cancers: new lessons from the IARC TP53 database and genomics data. *Hum Mutat* 2016, 37: 865–876
39. Wolf D, Harris N, Rotter V. Reconstitution of p53 expression in a nonproducer Ab-MuLV-transformed cell line by transfection of a functional p53 gene. *Cell* 1984, 38: 119–126
40. Zhang Y, Coillie SV, Fang JY, Xu J. Gain of function of mutant p53: R282W on the peak? *Oncogenesis* 2016, 5: e196
41. Hsiao M, Low J, Dorn E, Ku D, Pattengale P, Yeargin J, Haas M. Gain-of-function mutations of the p53 gene induce lymphohematopoietic metastatic potential and tissue invasiveness. *Am J Pathol* 1994, 145: 702–714
42. Lányi Á, Deb D, Seymour RC, Ludes-Meyers JH, Subler MA, Deb S. Gain of function phenotype of tumor-derived mutant p53 requires the oligomerization/nonsequence-specific nucleic acid-binding domain. *Oncogene* 1998, 16: 3169–3176
43. Georgakilas AG, Martin OA, Bonner WM. P21: a two-faced genome guardian. *Trends Mol Med* 2017, 23: 310–319
44. Khoury MP, Bourdon JC. P53 isoforms: an intracellular microprocessor? *Genes Cancer* 2011, 2: 453–465
45. Xu R, Yu S, Zhu D, Huang X, Xu Y, Lao Y, Tian Y, *et al.* hCINAP regulates the DNA-damage response and mediates the resistance of acute myelocytic leukemia cells to therapy. *Nat Commun* 2019, 10: 3812
46. Ando K, Parsons MJ, Shah RB, Charendoff CI, Paris SL, Liu PH, Fassio SR, *et al.* NPM1 directs PIDDosome-dependent caspase-2 activation in the nucleolus. *J Cell Biol* 2017, 216: 1795–1810
47. Sidi S, Bouchier-Hayes L. Direct pro-apoptotic role for NPM1 as a regulator of PIDDosome formation. *Mol Cell Oncol* 2017, 4: e1348325
48. Rogakou EP, Pilch DR, Orr AH, Ivanova VS, Bonner WM. DNA double-stranded breaks induce histone H2AX phosphorylation on serine 139. *J Biol Chem* 1998, 273: 5858–5868
49. Faivre S, Chan D, Salinas R, Woynarowska B, Woynarowski JM. DNA strand breaks and apoptosis induced by oxaliplatin in cancer cells. *Biochem Pharmacol* 2003, 66: 225–237
50. Abdeahad H, Avan A, Pashirzad M, Khazaei M, Soleimanpour S, Ferns GA, Fiuji H, *et al.* The prognostic potential of long noncoding RNA HOTAIR expression in human digestive system carcinomas: A meta-analysis. *J Cell Physiol* 2019, 234: 10926–10933
51. Wang W, He X, Zheng Z, Ma X, Hu X, Wu D, Wang M. Serum HOTAIR as a novel diagnostic biomarker for esophageal squamous cell carcinoma. *Mol Cancer* 2017, 16: 75
52. Ge XS, Ma HJ, Zheng XH, Ruan HL, Liao XY, Xue WQ, Chen YB, *et al.* HOTAIR, a prognostic factor in esophageal squamous cell carcinoma, inhibits WIF-1 expression and activates Wnt pathway. *Cancer Sci* 2013, 104: 1675–1682
53. Yang C, Li F, Zhou W, Huang J. Knockdown of long non-coding RNA CCAT2 suppresses growth and metastasis of esophageal squamous cell carcinoma by inhibiting the β-catenin/WISP1 signaling pathway. *J Int Med Res* 2021, 49: 030006052110199
54. Zhang X, Xu Y, He C, Guo X, Zhang J, He C, Zhang L, *et al.* Elevated expression of CCAT2 is associated with poor prognosis in esophageal squamous cell carcinoma. *J Surg Oncol* 2015, 111: 834–839
55. Rau R, Brown P. Nucleophosmin (*NPM1*) mutations in adult and childhood acute myeloid leukaemia: towards definition of a new leukaemia entity. *Hematol Oncol* 2009, 27: 171–181
56. Falini B, Nicoletti I, Bolli N, Martelli MP, Liso A, Gorello P, Mandelli F, *et al.* Translocations and mutations involving the nucleophosmin (NPM1) gene in lymphomas and leukemias. *Haematologica* 2007, 92: 519–532
57. Nozawa Y, Van Belzen N, Van Der Made ACJ, Dinjens WNM, Bosman FT. Expression of nucleophosmin/B23 in normal and neoplastic colorectal mucosa. *J Pathol* 1996, 178: 48–52
58. Yu ACY, Chern YJ, Zhang P, Pasiliao CC, Rahman M, Chang G, Ren J, *et al.* Inhibition of nucleophosmin 1 suppresses colorectal cancer tumor growth of patient -derived xenografts via activation of p53 and inhibition of AKT. *Cancer Biol Ther* 2021, 22: 112–123
59. Wong JCT, Hasan MR, Rahman M, Yu AC, Chan SK, Schaeffer DF, Kennecke HF, *et al.* Nucleophosmin 1, upregulated in adenomas and cancers of the colon, inhibits p53-mediated cellular senescence. *Int J Cancer* 2013, 133: 1567–1577
60. Wang X, Hu X, Song W, Xu H, Xiao Z, Huang R, Bai Q, *et al.* Mutual

dependency between lncRNA LETN and protein NPM1 in controlling the nucleolar structure and functions sustaining cell proliferation. *Cell Res* 2021, 31: 664–683

61. Zhang Y, Wolf GW, Bhat K, Jin A, Allio T, Burkhart WA, Xiong Y. Ribosomal protein L11 negatively regulates oncoprotein MDM2 and mediates a p53-dependent ribosomal-stress checkpoint pathway. *Mol Cell Biol* 2003, 23: 8902–8912
62. Bursać S, Brdovčak MC, Pfannkuchen M, Orsolić I, Golomb L, Zhu Y, Katz C, *et al.* Mutual protection of ribosomal proteins L5 and L11 from degradation is essential for p53 activation upon ribosomal biogenesis stress. *Proc Natl Acad Sci USA* 2012, 109: 20467–20472
63. Donati G, Peddigari S, Mercer CA, Thomas G. 5S ribosomal RNA is an essential component of a nascent ribosomal precursor complex that regulates the Hdm2-p53 checkpoint. *Cell Rep* 2013, 4: 87–98
64. Liu Q, Liu N, Shangguan Q, Zhang F, Chai W, Tong X, Zhao X, *et al.* LncRNA SAMD12-AS1 promotes cell proliferation and inhibits apoptosis by interacting with NPM1. *Sci Rep* 2019, 9: 11593
65. Korgaonkar C, Hagen J, Tompkins V, Frazier AA, Allamargot C, Quelle FW, Quelle DE. Nucleophosmin (B23) targets ARF to nucleoli and inhibits its function. *Mol Cell Biol* 2005, 25: 1258–1271
66. Lee C, Smith BA, Bandyopadhyay K, Gjerset RA. DNA damage disrupts the p14ARF-B23(nucleophosmin) interaction and triggers a transient subnuclear redistribution of p14ARF. *Cancer Res* 2005, 65: 9834–9842
67. Huang W, Deng B, Wang RW, Tan QY, Jiang YG. Expression of breast cancer anti-estrogen resistance 1 in relation to vascular endothelial growth factor, p53, and prognosis in esophageal squamous cell cancer. *Dis Esophagus* 2013, 26: 528–537
68. Tang Q, Efe G, Chiarella AM, Leung J, Chen M, Yamazoe T, Su Z, *et al.* Mutant p53 regulates survivin to foster lung metastasis. *Genes Dev* 2021, 35: 528–541
69. Grugan KD, Vega ME, Wong GS, Diehl JA, Bass AJ, Wong KK, Nakagawa H, *et al.* A common p53 mutation (R175H) activates c-Met receptor tyrosine kinase to enhance tumor cell invasion. *Cancer Biol Ther* 2013, 14: 853–859
70. Yao J, Zhang H, Li H, Qian R, Liu P, Huang J. P53-regulated lncRNA uc061hsf.1 inhibits cell proliferation and metastasis in human esophageal squamous cell cancer. *IUBMB Life* 2020, 72: 401–412
71. Iyer SV, Parrales A, Begani P, Narkar A, Adhikari AS, Martinez LA, Iwakuma T. Allele-specific silencing of mutant p53 attenuates dominant-negative and gain-of-function activities. *Oncotarget* 2016, 7: 5401–5415
72. Zhu HB, Yang K, Xie YQ, Lin YW, Mao QQ, Xie LP. Silencing of mutant p53 by siRNA induces cell cycle arrest and apoptosis in human bladder cancer cells. *World J Surg Onc* 2013, 11: 22
73. Huarte M, Guttman M, Feldser D, Garber M, Koziol MJ, Kenzelmann-Broz D, Khalil AM, *et al.* A large intergenic noncoding RNA induced by p53 mediates global gene repression in the p53 response. *Cell* 2010, 142: 409–419
74. Marín-Béjar O, Marchese FP, Athie A, Sánchez Y, González J, Segura V, Huang L, *et al.* Pint lincRNA connects the p53 pathway with epigenetic silencing by the Polycomb repressive complex 2. *Genome Biol* 2013, 14: R104
75. Dimitrova N, Zamudio JR, Jong RM, Soukup D, Resnick R, Sarma K, Ward AJ, *et al.* LincRNA-p21 activates p21 in cis to promote polycomb target gene expression and to enforce the G1/S checkpoint. *Mol Cell* 2014, 54: 777–790
76. Chen J, Zhu M, Zou L, Xia J, Huang J, Deng Q, Xu R. Long non-coding RNA LINC-PINT attenuates paclitaxel resistance in triple-negative breast cancer cells via targeting the RNA-binding protein NONO. *Acta Biochim Biophys Sin* 2020, 52: 801–809
77. Adriaens C, Standaert L, Barra J, Latil M, Verfaillie A, Kalev P, Boeckx B, *et al.* p53 induces formation of NEAT1 lncRNA-containing paraspeckles that modulate replication stress response and chemosensitivity. *Nat Med* 2016, 22: 861–868
78. Hung T, Wang Y, Lin MF, Koegel AK, Kotake Y, Grant GD, Horlings HM, *et al.* Extensive and coordinated transcription of noncoding RNAs within cell-cycle promoters. *Nat Genet* 2011, 43: 621–629
79. Schmitt AM, Garcia JT, Hung T, Flynn RA, Shen Y, Qu K, Payumo AY, *et al.* An inducible long noncoding RNA amplifies DNA damage signaling. *Nat Genet* 2016, 48: 1370–1376
80. Hu WL, Jin L, Xu A, Wang YF, Thorne RF, Zhang XD, Wu M. GUARDIN is a p53-responsive long non-coding RNA that is essential for genomic stability. *Nat Cell Biol* 2018, 20: 492–502
81. Wei CL, Wu Q, Vega VB, Chiu KP, Ng P, Zhang T, Shahab A, *et al.* A global map of p53 transcription-factor binding sites in the human genome. *Cell* 2006, 124: 207–219
82. Box JK, Paquet N, Adams MN, Boucher D, Bolderson E, O'Byrne KJ, Richard DJ. Nucleophosmin: from structure and function to disease development. *BMC Mol Biol* 2016, 17: 19
83. Bailey GD, Qutob HMH, Akhtar A, Russell NH, Seedhouse CH. DNA damage corrects the aberrant cytoplasmic localisation of nucleophosmin in NPM1 mutated acute myeloid leukaemia. *Br J Haematol* 2019, 186: 343–347
84. Sun C, Gao Y, Yang L, Shao H, li J, Gao X, Ma L, *et al.* NPM1A in plasma is a potential prognostic biomarker in acute myeloid leukemia. *Open Life Sci* 2018, 13: 236–241
85. Brown P, McIntyre E, Rau R, Meshinchi S, Lacayo N, Dahl G, Alonzo TA, *et al.* The incidence and clinical significance of nucleophosmin mutations in childhood AML. *Blood* 2007, 110: 979–985
86. Falini B, Nicoletti I, Martelli MF, Mecucci C. Acute myeloid leukemia carrying cytoplasmic/mutated nucleophosmin (NPMc+ AML): biologic and clinical features. *Blood* 2007, 109: 874–885